separation of silicates from residual carbonates with 500 μl of ~8 M acetic acid in an ultrasonic bath (~10 min) and on a warm hotplate (~15 min) with a 500-μl rinse of water in between. Subsequently, the sample was leached with warm 2.5 M HCl for ~5 min, followed by another rinse with 500 μl of water. All leachates and rinses were collected and analyzed; they contained ≤6‰ of Sr that previously resided in the silicates. After addition of a ^{84}Sr-^{85}Rb tracer, the silicate samples were dissolved in closed fluorinated ethylene propylene (FEP) vials at ~80°C with 400 μl of concentrated HF and 10 μl of concentrated HNO_3 (3 days) and equilibrated with 400 μl of 6M HCl overnight. The solutions were scrutinized with a binocular microscope and found to be free of undissolved particles or precipitates. Carbonate samples were dissolved with 500 μl of ~8 M acetic acid. All sample weights of PFC-2 and the silicate sample weights of PFC-1 are given according to the estimated modal abundances deduced from thick section. Measured values for the SRM987 Sr standard were 0.710292 ± 13 (1σ; static mode Faraday; 10 to 100 ng of Sr; $n = 23$).

4. J. G. Ramsay and M. I. Huber, *The Techniques of Modern Structural Geology*, vol. 1, *Strain Analysis* (Academic Press, London, 1983).
5. D. Dietrich, *Tectonophysics* **170**, 183 (1989).
6. D. Fischer and T. Byrne, *Tectonics,* **11**, 330 (1992).
7. D. G. A. M. Aerden, *J. Struct. Geol.* **18**, 75 (1996).
8. J.-L. Olivet, *Bull. Cent. Rech. Explor. Prod. Elf Aquitaine* **20**, 131 (1996).
9. W. R. Roest and S. P. Srivastava, *Geology* **19**, 613 (1991).
10. P. Choukroune, *Annu. Rev. Earth Planet. Sci.* **20**, 143 (1992).
11. J.-M. Goldberg and H. Maluski, *C. R. Acad. Sci. Ser. II* **306**, 429 (1988).
12. A deformation phase is defined as a time interval with a constantly oriented stress field. The distinction of D1, D2, and D3 deformation phases at Lourdes is based on field investigations and microstructural analysis revealing a superposition of three tectonic foliations (S1, S2, and S3), as well as geometric modeling of PFCs yielding hook-shaped pyrite-center trajectories parallel to S2 and S3 (*7*).
13. W. Müller, R. D. Dallmeyer, F. Neubauer, M. Thöni, *J. Geol. Soc. London* **156**, 261 (1999).
14. L. J. Garwin, thesis, Cambridge University (1985).
15. On the basis of kinematic reconstruction (Fig. 4), D2 strains were measured by the change in length (Δl) of a line (l_0) connecting the external terminations of opposite fringes (strain = $\Delta l/l_0$). D3 strains were calculated by treating the pre-D3 PFC as three rigid fragments being pulled apart (as normal boudinage), whereby the gap between fragments is filled by D3 fibers. D3 strain corresponds to the length change of a line connecting the midpoints of the original D2 fringes. Microsamples were cut according to the shape of successive D2 and D3 growth increments. They represent time intervals, so their ages correspond to about their median line, although the older half represents slightly more strain than the younger half (l_0 differs for both). This difference was taken into account for calculation of the dated strains (Table 2). Quantitative errors in this procedure are negligible because length changes can be measured very precisely. Qualitative errors in the (manual) kinematic reconstruction are considered small as seen from the close match between true and modeled fibers (Figs. 1 and 2).
16. S. R. Freeman, S. Inger, R. W. H. Butler, R. A. Cliff, *Tectonics* **16**, 57 (1997).
17. J. G. Ramsay, *Nature* **284**, 135 (1980).
18. We thank N. Mancktelow for discussions, T. Willi for thick-section preparation, and M. Meier for lab support. Reviews by two anonymous reviewers and comments by D. Dietrich, J. G. Ramsay, and A. B. Thompson helped to improve the manuscript and are gratefully acknowledged.

19 January 2000; accepted 11 April 2000

Coherent High- and Low-Latitude Climate Variability During the Holocene Warm Period

Peter deMenocal,[1]* Joseph Ortiz,[1] Tom Guilderson,[2] Michael Sarnthein[3]

A faunal record of sea-surface temperature (SST) variations off West Africa documents a series of abrupt, millennial-scale cooling events, which punctuated the Holocene warm period. These events evidently resulted from increased southward advection of cooler temperate or subpolar waters to this subtropical location or from enhanced regional upwelling. The most recent of these events was the Little Ice Age, which occurred between 1300 to 1850 A.D., when subtropical SSTs were reduced by 3° to 4°C. These events were synchronous with Holocene changes in subpolar North Atlantic SSTs, documenting a strong, in-phase link between millennial-scale variations in high- and low-latitude climate during the Holocene.

The warm climate of the Holocene epoch [the last 11,700 thousand years (11.7 ky B.P.)] conventionally has been viewed as climatically stable (*1*) with little evidence of the abrupt millennial-scale climatic shifts that characterize glacial periods (*2*, *3*). Oxygen isotopic records from central Greenland ice cores indicate essentially no Holocene variability, with the notable exception of the Preboreal and early Holocene cooling events near 10 and 8.2 thousand years ago (ka) (*4*). However, recently developed Holocene paleoclimate records from ice cores and high-latitude marine sediments show that Holocene climate was also unstable, having been punctuated by several significant, millennial-scale cooling events, which recurred roughly every 1500 ± 500 years (*5*–*8*). The most recent of these Holocene cooling events was the Little Ice Age between ca. 1300 to 1870 A.D. (*5*, *9*), when Scandinavian glaciers attained their furthest expansion since 9 ka (*10*).

Unlike for high latitudes, little is known about the possibility of such millennial-scale climate variability in lower latitudes. Furthermore, the mechanisms underlying this variability remain unclear. Understanding this mode of climate variability is particularly relevant because it represents a natural, recurrent climatic instability, which evidently operates independently of the size of high-latitude ice sheets as these ~1500-year cooling events occurred during both glacial and interglacial climatic extrema (*7*). Here we investigate the timing, amplitude, and nature of low-latitude climate variability during the Holocene, and demonstrate that high- and low-latitude climates were coupled by quantifying past SST variations preserved in a well-dated, high-accumulation-rate sediment core off West Africa.

Ocean Drilling Program Hole 658C was cored off Cap Blanc, Mauritania (20°45′N, 18°35′W; 2263 m water depth) (*11*) during the Ocean Drilling Program (ODP) Leg 108 (Fig. 1). Sediment accumulation rates are high at this site (22 cm/ky average) due, in part, to the dual influences of high regional surface ocean productivity and high supply of windblown African mineral dust. Strong seasonal upwelling and high productivity results from the strong northeast trade winds, which parallel the Northwest African margin (*12*). Hole 658C is also positioned within the axis of the summer African eolian dust plume (Fig. 1), which transports Saharan mineral aerosol dust to the adjacent subtropical Atlantic Ocean (*13*). The site is well situated to monitor past changes in regional ocean circulation because it lies within an oceanographic boundary separating cooler temperate and subpolar waters to the north from warmer tropical water masses to the south and west (Fig. 1).

Core 1H from Hole 658C was continuously subsampled at 2-cm intervals, which is equivalent to between 50 and 100 years temporal resolution. Samples were analyzed for calcium carbonate and biogenic opal percent-

[1]Lamont-Doherty Earth Observatory of Columbia University, Palisades, NY 10964, USA. [2]Center for Accelerator Mass Spectrometry, Lawrence-Livermore National Laboratory, Livermore, CA 94551, USA. [3]Institut für Geowissenschaften, Universität Kiel, Kiel, Germany.

*To whom correspondence should be addressed. E-mail: peter@ldeo.columbia.edu

ages, and the residual terrigenous (eolian) fraction was computed by difference. Planktonic foraminiferal assemblage census counts were then conducted on prepared samples (*14*). Warm and cold season SST estimates were calculated from the census count data using the F13′ transfer function derived from faunal analysis of 191 Atlantic core tops (*15*, *16*). Standard errors of estimate for the F13′-derived warm and cold season SSTs are 1.6° and 1.3°C, respectively. At Hole 658C, the coretop (0 to 2 cm) warm and cold season foraminiferal SST estimates (16.8° and 25.8°C, respectively) agree within the error of estimate with the observed annual SST range at this location (18° and 24°C, respectively) (Fig. 2).

Age control was established with 31 accelerator mass spectrometer (AMS) radiocarbon dates of monospecific samples of planktonic foraminifera (*Globigerina bulloides* or *Globorotalia inflata*) spanning the last 24 ky (*17*) (Fig. 2). Raw radiocarbon dates were converted to calibrated calendar ages after applying a −500 ± 50 year reservoir correction (*18*, *19*). The resulting age-depth profile (Fig. 2) indicates that sedimentation was continuous at a rate of 22 cm/ka spanning the last ~14 ky. However, a brief hiatus between 328 and 324 cm (17.4 to 14.3 ka) is indicated by several closely spaced dates (*20*) (Fig. 2).

The reconstructed SST variations demonstrate that the Holocene interval at subtropical Atlantic Hole 658C was punctuated by numerous discrete, millennial-scale cooling events (Figs. 2 and 3). Using our calibrated radiocarbon ages, we defined a succession of Holocene cooling events centered at 10.2, 8.0, 6.0, 4.6, 3.0, and 1.9 ka, as well as two closely spaced but discrete events in the most recent part of the record at 0.80 and 0.35 ka (Fig. 3). The Holocene subtropical cooling events are large: The peak Holocene cooling at ~8.0 ka (~7° to 8°C) (Figs. 2 and 3) was equivalent to the cooling that occurred here

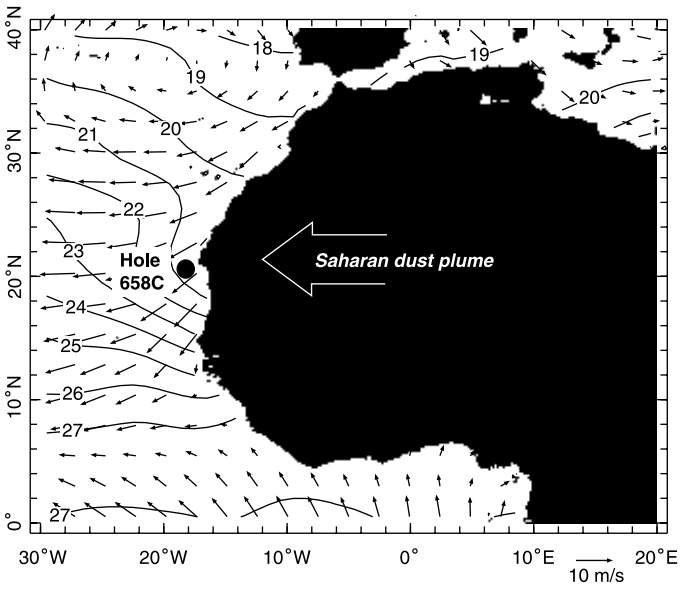

Fig. 1. Location of the ODP Hole 658C off Cap Blanc, West Africa. Arrows depict the boreal winter surface wind field and the contours indicate the annual mean SST values. Sea-surface temperature (SST) seasonality is high at this location (18° to 24°C; 21°C is the annual mean) due to the seasonal wind-driven upwelling of cold, nutrient-rich waters along the West African coast (*12*). High sedimentation rates (22 cm/ka) result from the dual influences of high surface productivity and high influx of Saharan mineral dust (*13*), which is transported westward near 22°N by the African Easterly Jet (*13*).

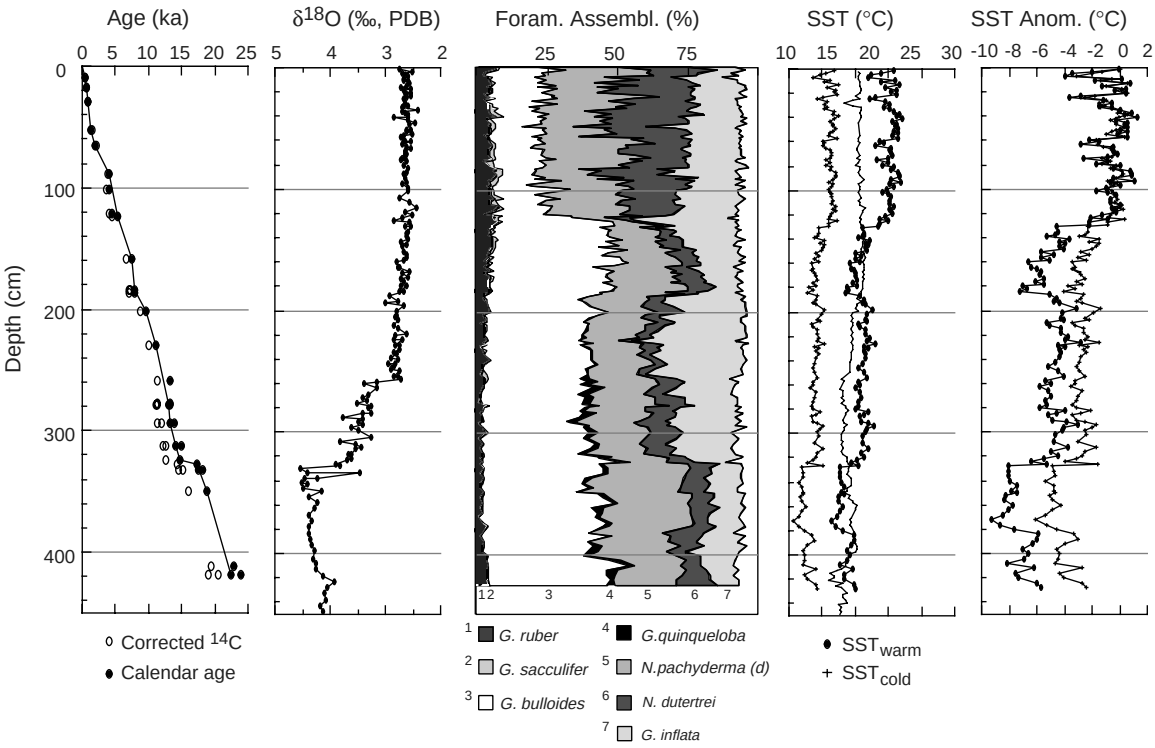

Fig. 2. The AMS radiocarbon age model, benthic (*Cibicides wuellerstorfi*) oxygen isotope stratigraphy, planktonic foraminiferal census data, and the calculated transfer function estimates of warm- and cold-season SST variations at Hole 658C. Age control was established by 31 AMS radiocarbon dates on *G. bulloides* (or *G. inflata)* spanning the last 24 ky, and a brief hiatus between 14.8 to 17.2 ka (324 cm to 328 cm) is indicated by several closely spaced dates (*17*). Warm (SST_{warm}) and cold (SST_{cold}) season estimates were calculated with the F13′ transfer function applied to the foraminiferal census data (*16*), which has standard errors of estimate of 1.6° and 1.3°C, respectively. Alkenone-derived SST estimates from Hole 658C are shown by the solid line without symbols (*27*). The warm and cold season SST anomalies relative to coretop values are also shown. The numerous Holocene cool events (~2° to 4°C amplitude) can be attributed to marked increases in the abundances of the subpolar species *N. pachyderma* (right-coiling) and decreases in the temperate or transitional species *G. inflata*, suggesting enhanced delivery of cool subpolar waters during these events. Increased upwelling is also associated with the early Holocene cool events, as documented by the large increase in *G. bulloides* abundance before 5.5 ka (125 cm). The order of the species represented in the middle panel follow in numerical sequence as indicated below that panel.

during the last glacial maximum (*15*, *21*).

These subtropical Atlantic, millennial-scale cooling events recurred about every 1500 ± 500 years, which is indistinguishable from the 1470 ± 500 year recurrence interval of Holocene and late glacial climate instabilities documented for the North Atlantic (*7*, *8*). Furthermore, the timing of the subtropical Holocene cool events closely match those identified in three North Atlantic sediment cores (*7*, *9*) (Fig. 3), although timing offsets are possible within the dating uncertainty (±100 to 200 years). In comparing the full suite of Holocene cooling events, we do not detect any systematic temporal offsets between the subpolar and subtropical Atlantic within the calibrated radiocarbon chronologies. The maximum Holocene SST cooling at Hole 658C near 8.0 ka was evidently synchronous with a well-documented high-latitude cooling event that resulted from the terminal collapse of a remnant Laurentide ice mass near Hudson Bay. This early Holocene cooling had a near-global impact (*4*) and was associated with cooler, drier conditions in subtropical West Africa (*22*). Holocene Event 6 (~9.5 ka), as defined by Bond and colleagues (*7*), was not resolved at Hole 658C, evidently due to a brief interval of lowered accumulation rates (Figs. 2 and 3).

The Little Ice Age (LIA) was the most recent of these millennial-scale Holocene cooling events (*5*, *7*, *9*). Historical records have suggested that the LIA was composed of at least two discrete cooling periods (*23*). Reconstruction of past Greenland surface temperature variations with glacier borehole temperature data document two discrete LIA cooling events centered at ~1500 and ~1850 A.D. (*24*) (Fig. 4). At Hole 658C, the LIA cooling is also represented by two distinct 3° to 4°C cooling events between ~1300 and 1900 A.D.; the earlier Medieval Warm Period (MWP), between ~400 and 1000 A.D., was only marginally warmer than present (Fig. 4). Oxygen isotopic analyses of planktonic foraminifera in a well-dated, high-deposition-rate sediment core from the Bermuda Rise (*25*) also document a two-event, 1°C LIA cooling (Fig. 4) that was preceded by the WMP, which was about 1°C warmer. These records collectively indicate that, within the respective dating uncertainties (±100 years, 2 σ), the subpolar and subtropical North Atlantic experienced a comparable succession of warming and cooling events during the latest Holocene.

The faunal assemblage variations at Hole 658C indicate that the Holocene cold events reflect the dual influences of increased southward advection of colder subpolar waters and enhanced regional upwelling. Four planktonic foraminifera species account for nearly 90% of the total assemblage variability at Hole 658C [temperate or subtropical forms *G. inflata* and *Neogloboquadrina dutertrei* and subpolar forms *Neogloboquadrina pachyderma* (right-coiling) and *G. bulloides*]. The observed millennial-scale SST variations can be attributed to abundance variations between two main forms (Fig. 2): *N. pachyderma* (right-coiling), which has maximum abundances in subpolar waters near 10°C (*15*), and *G. inflata*, which is a transitional species associated with warmer Gulf Stream waters near 18°C (*15*). We attribute the millennial-scale SST variations to changes in the relative strength of the eastern boundary Canary Current, which presently advects temperate or subpolar waters along the western European margin to the West African coast. A similar interpretation was reached for the last glacial maximum (LGM) cooling off West Africa based on the faunal and SST changes observed in the subtropical east Atlantic (*15*, *21*, *26*). However, alkenone-derived SST reconstructions at Hole 658C do not indicate these large SST variations during the Holocene (*27*), with the notable exception of the LIA cooling (Fig. 2), and they tend to underestimate the LGM cooling relative to the faunal estimates. Differences between faunal and alkenone SST reconstructions have been described in detail for this same

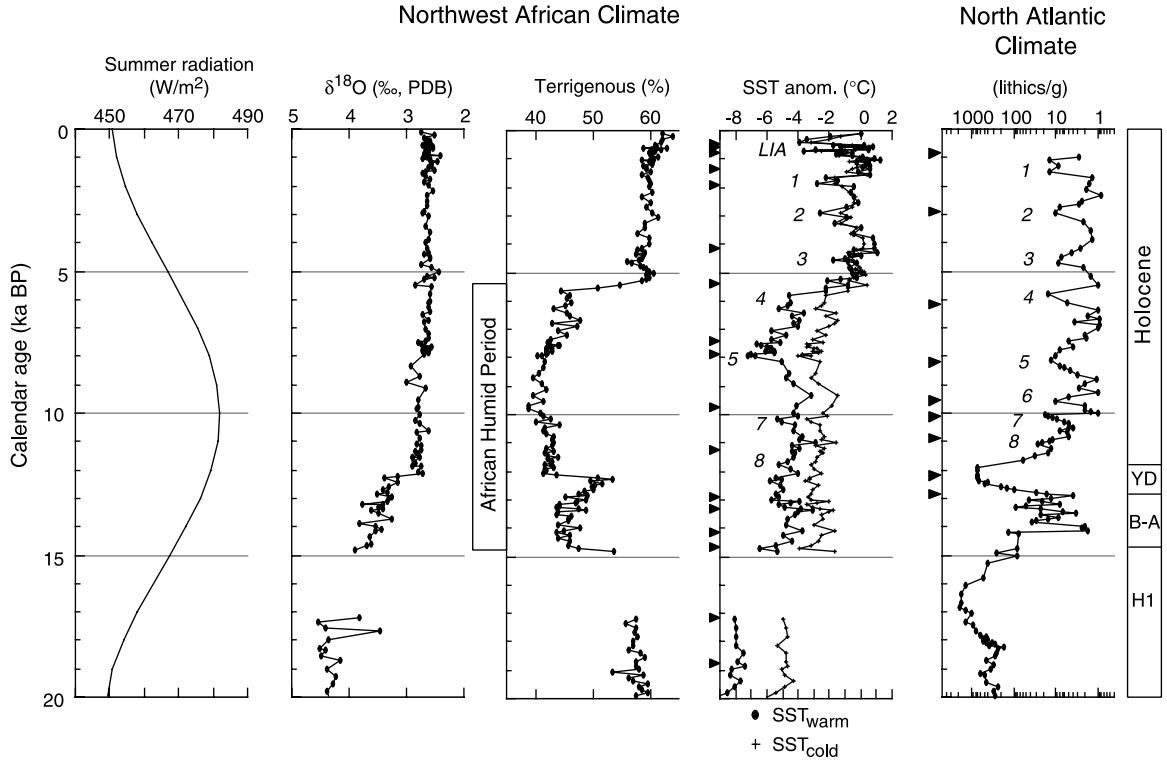

Fig. 3. Late Glacial to Holocene variations in West African climate and subtropical Atlantic SST from Hole 658C compared with a record of glacial ice-rafted lithic grain concentrations from subpolar North Atlantic core V29-191 (*7*). Calibrated radiocarbon age control points for both records are indicated by filled arrow symbols. The Hole 658C SST record documents a series of millennial-scale cooling events of 2° to 4°C amplitude, which are coherent with the Holocene series of North Atlantic ice-rafting events defined by Bond *et al.* (*7*) within the dating uncertainties (±100 years). These millennial-scale SST variations were superimposed on a well-known shift in African monsoonal climate between 14.8 and 5.5 ka, when changes in the earth's orbit increased boreal summer insolation and invigorated the African monsoon, bringing much wetter conditions to subtropical Africa (*28*). The strengthened monsoonal wind field evidently supported stronger upwelling as documented by the greatly increased *G. bulloides* abundances (Fig. 2). The reduced terrigenous (eolian) concentrations at Hole 658C document the abrupt onset and termination of the African Humid Period at 14.8 and 5.5 ka, respectively, and reflect the increased humidity of African dust source areas at this time, when subtropical West Africa was nearly completely vegetated (*20*, *29*).

area (*26*) and have been related to shifts in the dominant upwelling season.

The faunal SST reconstructions also indicate that the seasonal SST range (warm- minus cold-season SST) was greatly reduced during these Holocene cool events. Reconstructed warm-season (summer) SSTs cooled significantly more than the cool-season (winter) SSTs, resulting in a reduction in the seasonal SST range during cool events (Fig. 2). Consequently, there is a very strong correspondence between changes in warm-season temperature (SST_{warm}) and changes in SST seasonality [$r^2 = 0.90$; seasonality $= 0.45(SST_{warm}) - 2.6$]. Hydrographically, the cool events would be associated with a suppression of the summer-season warming, which at present occurs in this region because of the seasonal weakening of trade-wind upwelling and the northward migration of warmer tropical surface waters. The reduced seasonality suggests that the cool SSTs occurred throughout the year during these cool events, supporting the view that they reflected enhanced eastern boundary current delivery of cooler subpolar waters or increased regional upwelling.

These millennial-scale SST variations were superimposed upon a well-known change in subtropical African climate, which occurred between 14.8 and 5.5 ka. The reduced terrigenous eolian percentage values during that time (Fig. 3) reflect a period of greatly increased rainfall and vegetation cover in the now hyperarid Saharan desert known as the African Humid Period (*28*), when subtropical North Africa was nearly completely vegetated (*29*) and supported abundant savannah and lake margin fauna such as antelope, giraffe, elephant, hippopotamus, crocodile, and human settlements in regions that today have almost no measurable precipitation. The mass flux of eolian terrigenous sediment supply at Hole 658C was reduced by 47% during the African Humid Period relative to modern values (*20*). The lowered SST values during this period are attributed to increased regional upwelling and productivity, as evidenced by the greatly increased percentages of the upwelling-indicator species *G. bulloides* (*15*) (Fig. 2) and increased foraminifera per gram values (*30*). The African Humid Period was punctuated by a brief return to much more arid conditions during the Younger Dryas event (*22*), as recorded by the increased terrigenous (eolian) percentage values (Fig. 3).

The early Holocene greening of North Africa has been linked to an intensification of the African monsoon due to Earth orbital changes. By 10 to 11 ka, summer insolation in the Northern Hemisphere had risen to peak levels about 8% greater than today due to orbital precession that gradually aligned boreal summer solstice with the perihelion (Fig. 3). The early Holocene increase in boreal summer radiation promoted a much stronger monsoonal circulation, an observation supported by abundant paleoclimate data (*19*, *22*, *29*) and climate model results (*31*). The transitions into (at 14.8 ka) and out of (at 5.5 ka) the African Humid Period were very abrupt, occurring within a few centuries or less (Fig. 3) (*20*), which confirms other paleoclimate results (*22*, *29*) that document the very rapid and abrupt monsoonal climate response to gradual orbital radiation forcing. Why were the monsoonal climate responses so rapid? Recent fully coupled climate model simulations have shown that African climate can switch abruptly (within decades) between "wet" and "dry" conditions due to vegetation-albedo positive feedback effects that amplify the insolation-driven changes in monsoonal climate (*32*).

The results from Hole 658C document that the sequence of Holocene climate instabilities recognized in Greenland and in the subpolar North Atlantic are also detected in the subtropical Atlantic. This millennial-scale mode of Holocene climate instability appears to have been roughly synchronous across the North Atlantic basin, including the subpolar (*6–9*), temperate (*25*), and subtropical regions. This view differs from the latest Holocene SST results described by Keigwin and Pickart (*33*), who suggest that the Laurentian Fan sector of the northwest Atlantic actually warmed during the Little Ice Age (*33*), resembling a pattern associated with North Atlantic Oscillation (NAO). Interannual variations in eastern North Atlantic subtropical SSTs are also significantly correlated to the NAO (*34*) and occur at the same phasing with respect to the NAO index as the region studied by Keigwin and Pickart (*33*), so the Hole 658C data provide an additional data set for testing whether these millennial-scale SST variations were out of phase with the subpolar North Atlantic results (*7*, *9*). We do not detect any systematic SST phase offsets between paleoceanographic records from the Atlantic subpolar, temperate, or subtropical regions (Figs. 3 and 4).

Whatever their ultimate cause, these millennial-scale Holocene SST variations appear to have involved the entire North Atlantic basin (*6–9*, *25*), recurred with a ~1500 ± 500 year period throughout glacial and interglacial intervals (*6–9*), were accompanied by terrestrial climate changes (*19*, *22*, *29*), and involved large-scale ocean and atmosphere reorganizations that were completed within decades or centuries, perhaps less (*35*). These climate perturbations continue to persist during "our time." The most recent of these, the LIA, ended in the late 19th century, and some of the warming since that time may be related to the present warming phase of this millennial-scale climate oscillation (Fig. 4), although the warming in recent decades is unprecedented relative to the past millennium (*36*). The Hole 658C SST record also supports the view that Holocene climate variability has been increasing in recent millennia (*37*), with the LIA representing the largest-amplitude event of the last 20 ky (Fig. 3). These results underscore the need to understand anthropogenic warming within the context of rates and amplitudes of natural late Holocene climate variability.

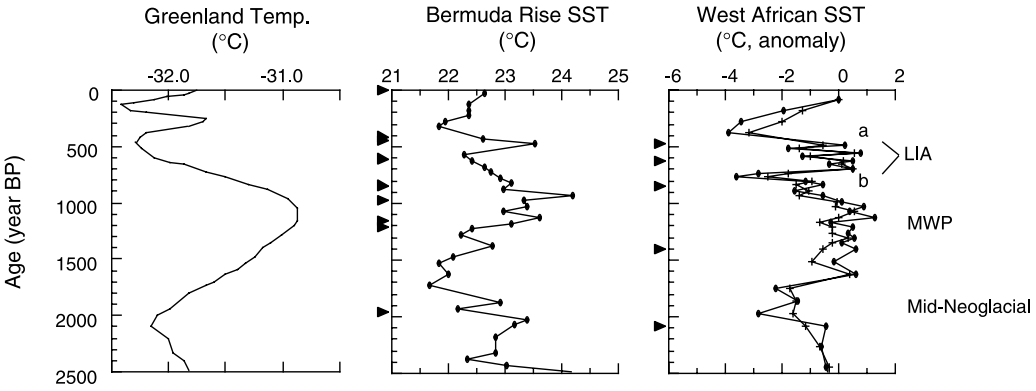

Fig. 4. High-resolution records of the last millennial-scale climate cycle spanning the MWP (occurring between 800 and 1300 A.D.) and the LIA (which occurred between 1300 and 1870 A.D.) (*23*) from Greenland (*24*), the western North Atlantic (*25*), and the eastern subtropical North Atlantic (Hole 658C). The record of Greenland surface temperature variations was reconstructed from glacier borehole temperature data (*24*) and documents two discrete LIA cooling events centered at ~1500 and ~1870 A.D. Oxygen isotopic analyses of planktonic foraminifera in a well-dated, high-deposition-rate sediment core from the Bermuda Rise (*25*) also document a twin-event, 1°C cooling signature of the LIA (Fig. 4) that was preceded by the MWP, which was about 1°C warmer. At Hole 658C, the LIA cooling is also indicated by two distinct cooling events of 3° to 4°C amplitude between ~1300 and 1850 A.D.; the earlier MWP between ~800 and 1200 A.D. was only marginally warmer than present. These results suggest that the most recent LIA-MWP climatic cycle occurred synchronously at these three locations within the dating uncertainties.

References and Notes

1. W. Dansgaard *et al.*, *Nature* **364**, 218 (1993).
2. G. Bond *et al.*, *Nature* **365**, 143 (1993).
3. W. S. Broecker, *Nature* **372**, 421 (1994).
4. R. B. Alley *et al.*, *Geology* **25**, 483 (1997).
5. G. H. Denton and W. Karlen, *Quat. Res.* **3**, 155 (1973).
6. S. R. O'Brien *et al.*, *Science* **270**, 1962 (1995).
7. G. Bond *et al.*, *Science* **278**, 1257 (1997).
8. G. G. Bianchi and I. N. McCave, *Nature* **397**, 515 (1999).
9. G. C. Bond *et al.*, in *Mechanisms of Global Climate Change at Millennial Scales*, P. U. Clark, R. S. Webb, L. D. Keigwin, Eds. (Geophysical Monograph Series, American Geophysical Union, Washington, D.C., 1999), vol. 12, pp. 35–58.
10. J. M. Grove, *The Little Ice Age* (Methuen, London, 1987).
11. W. Ruddiman, M. Sarnthein, J. Baldauf, Eds., *Proceedings of the Ocean Drilling Program Leg 108*, vol. A (ODP, College Station, TX, 1988).
12. G. Fischer, B. Donner, V. Ratmeyer, R. Davenport, G. Wefer, *J. Mar. Res.* **54**, 73 (1996).
13. L. Schütz, R. Jaenicke, H. Pietrek, *Geol. Soc. Amer. Bull. Spec. Pap.* **186**, 87 (1981).
14. Raw, freeze-dried samples of about 3 g were washed through a 64-μm sieve, dried, weighed, and then dry-sieved through a sieve with 150-μm openings. The >150-μm fraction was split a sufficient number of times to microscopically identify and count between 400 and 900 specimens per sample. This relatively large number of specimens was counted to ensure that counting uncertainties were minimized for the 29 identified species. The F13′ transfer function was used because it specifically addresses the "P-D intergrade" identification problem [a species present in these West African samples that is morphologically intermediate between *N. pachyderma* (dextral, or right coiling) and *N. dutertrei* (*15*, *16*)]. Computed average communalities for the estimated warm and cold SST values, which are a measure of how well the Hole 658C faunal assemblage data match the F13′ transfer function model, were uniformly high (0.82 was the average).
15. N. G. Kipp, in *Investigation of Late Quaternary Paleoceanography and Paleoclimatology*, R. M. Cline and J. D. Hays, Eds. (Geological Society of America, Boulder, CO, 1976), pp. 3–42.
16. W. F. Ruddiman and L. K. Glover, *Quat. Res.* **5**, 361 (1975).
17. Web table 1 is available at *Science* Online at www.sciencemag.org/feature/data/1048976.shl.
18. M. Stuiver *et al.*, *Radiocarbon* **40**, 1041 (1998).
19. AMS radiocarbon dates were conducted on monospecific samples of between 1000 to 1500 picked (>150 μm) specimens of the planktonic foraminifer *G. bulloides*. Samples were sonicated in deionized water before analysis and measurements were conducted at the Center for Accelerator Mass Spectrometry (CAMS) at the Lawrence Livermore National Laboratory and the University of Kiel, Germany. Raw radiocarbon ages were corrected for the global average surface ocean reservoir correction (–400 years) plus an additional –100 ± 50 year correction to reflect the higher and more variable surface ocean reservoir age of this upwelling region. Corrected radiocarbon ages were converted to calibrated, calendar ages with the Calib 4.12 program (*17*, *18*). Paired AMS dates on *G. bulloides* and *G. inflata* were conducted at seven levels to assess possible species offsets. These paired dates indicate that the *G. bulloides* ages were consistently older than *G. inflata* ages by several hundred years which we attribute to *G. bulloides*' known preference for calcifying during the main upwelling season when older subsurface waters are brought to the upper photic zone (*38*). The Hole 658C age model was based on the youngest measured age at any given stratigraphic level.
20. P. B. deMenocal *et al.*, *Quat. Sci. Rev.* **19**, 347 (2000).
21. A. C. Mix, W. F. Ruddiman, A. McIntyre, *Paleoceanography* **1**, 339 (1986).
22. F. Gasse and E. Van Campo, *Earth Planet. Sci. Lett.* **126**, 435 (1994).
23. P. D. Jones and R. S. Bradley, *Climate Since A.D. 1500* (Routledge, London, 1995).
24. D. Dahl-Jensen *et al.*, *Science* **282**, 268 (1998).
25. L. D. Keigwin, *Science* **274**, 1504 (1996).
26. M. R. Chapman, N. J. Shackleton, M. Zhao, G. Eglinton, *Paleoceanography* **11**, 343 (1996).
27. M. Zhao, N. A. S. Beveridge, N. J. Shackleton, M. Sanrthein, G. Eglinton, *Paleoceanography* **10**, 661 (1995).
28. F. A. Street and A. T. Grove, *Quat. Res.* **12**, 83 (1979).
29. COHMAP Members, *Science* **241**, 1043 (1988).
30. P. deMenocal, J. Ortiz, T. Guilderson, M. Sarnthein, data not shown.
31. W. L. Prell and J. E. Kutzbach, *J. Geophys. Res.* **92**, 8411 (1987).
32. M. Claussen *et al.*, *Geophys. Res. Lett.* **26**, 2037 (1999).
33. L. D. Keigwin and R. S. Pickart, *Science* **286**, 520 (1999).
34. J. W. Hurrell, *Science* **269**, 676 (1995).
35. R. B. Alley *et al.*, *Nature* **362**, 527 (1993).
36. M. E. Mann, J. Park, R. S. Bradley, *Nature* **392**, 7797 (1998).
37. E. J. Steig, *Science* **286**, 1485 (1999).
38. M. Sarnthein and G. Ganssen, in *Coastal Upwelling: Its Sediment Record*, E. Suess and J. Theide, Eds. (Plenum, New York, 1983), pp. 99–121.

39. The authors would like to thank J. Adkins, G. Bond, W. Broecker, B. Chaisson, M. Claussen, F. Gasse, L. Keigwin, G. Kukla, C. Ravelo, D. Rind, N. Shackleton, and J. Lynch-Steiglitz for insightful comments, stimulating discussions, and helpful criticisms. The foraminiferal census counts were conducted by M. Bryant and the sediment analyses were completed by L. Baker; A. Esmay assisted with the transfer function development. We also gratefully acknowledge J. Miller and P. Weiss of ODP who helped sample Hole 658C. Supported by NSF grant OCE-9818631. This is Lamont-Doherty Earth Observatory Publication Number 6066.

27 January 2000; accepted 3 May 2000

Nonavian Feathers in a Late Triassic Archosaur

Terry D. Jones,[1]* John A. Ruben,[1] Larry D. Martin,[2] Evgeny N. Kurochkin,[3] Alan Feduccia,[4] Paul F. A. Maderson,[5] Willem J. Hillenius,[6] Nicholas R. Geist,[7] Vladimir Alifanov[3]

Longisquama insignis **was an unusual archosaur from the Late Triassic of central Asia. Along its dorsal axis *Longisquama* bore a series of paired integumentary appendages that resembled avian feathers in many details, especially in the anatomy of the basal region. The latter is sufficiently similar to the calamus of modern feathers that each probably represents the culmination of virtually identical morphogenetic processes. The exact relationship of *Longisquama* to birds is uncertain. Nevertheless, we interpret *Longisquama*'s elongate integumentary appendages as nonavian feathers and suggest that they are probably homologous with avian feathers. If so, they antedate the feathers of *Archaeopteryx*, the first known bird from the Late Jurassic.**

Longisquama insignis was a small, Late Triassic [Norian, ~220 million years ago (Ma)], gliding archosaur with unusual integumentary appendages (*1*–*3*). Fossils are known only from lacustrine deposits in central Asia [Madygan, Osh Province, Kyrgyzstan (*1*, *2*)]. The most complete specimen consists of a slab and counterslab that contains articulated elements from the skull, vertebrae, ribs, furcula, and forelimbs and impressions of much of the integument (Fig. 1 and Web fig. 1). There are five other fossils of integumentary appendages from the same site (*1*, *4*).

The anterior portion of *Longisquama*'s body was covered with imbricating, scalelike appendages; those on the chin and neck were particularly delicate and elongate (Fig. 1, upper left inset). In addition, a series of scales (*1*) formed an apparent aerofoil-like surface along the postaxial margins of the forelimbs (Fig. 1, lower right inset). Most remarkable, however, are the series of six to eight pairs of bilaterally placed, markedly elongate, pinnate, integumentary appendages that occurred at segmental intervals along the animal's dorsum (Fig. 1 and Web fig. 1).

Longisquama's pinnate integumentary appendages each consisted of a distinct shaft that included a distally expanded vane. At its base, the elongate shaft was tubular, with a solid wall that surrounded a number of transverse partitions. Four to six of these partitions are visible in one particularly well-preserved shaft (Fig. 2). Additionally, as seen in three successive units immediately adjacent to the dorsal vertebrae, the broad, tubelike bases of the appendages were approximately barrel-shaped and tapered proximally—a morphology consistent with their placement within, and origin from, follicles (Fig. 2).

[1]Department of Zoology, Oregon State University, Corvallis, OR 97331, USA. [2]Museum of Natural History and Department of Ecology and Evolutionary Biology, University of Kansas, Lawrence, KS 66045, USA. [3]Palaeontological Institute, Russian Academy of Sciences, Moscow GSP-7, 117868, Russia. [4]Department of Biology, University of North Carolina, Chapel Hill, NC 27599, USA. [5]Department of Biology, Brooklyn College of the City University of New York, Brooklyn, NY 11210, USA. [6]Department of Biology, College of Charleston, Charleston, SC 29424, USA. [7]Department of Biology, Sonoma State University, Rohnert Park, CA 94928, USA.

*To whom correspondence should be addressed. Present address: Department of Biology, Stephen F. Austin State University, Nacogdoches, TX 75962, USA. E-mail: tdjones@sfasu.edu